

Vegetation Community Composition and Species–Environment Relationships Along an Elevational Gradient in South-Central Bhutan

Abstract

Questions: Understanding how plant communities vary along elevation is essential for predicting biodiversity responses to environmental change. We asked how community composition, diversity, and species–environment relationships differ among vegetation strata along an elevational gradient, and which environmental variables best explain regeneration patterns.

Location: Sarpang District, south-central Bhutan; unmanaged subtropical to cool broadleaved forests spanning approximately 260 to 1 964 m a.s.l.

Methods: We analysed vegetation data from four strata (trees, shrubs, herbs, regeneration) across 220 plots. We constructed community matrices, quantified environmental variables, applied non-metric multidimensional scaling and canonical correspondence analysis, and tested group differences with permutational multivariate analysis of variance. Indicator species analysis and machine-learning models (random forest and gradient boosting) assessed regeneration patterns.

Results: Community composition differed among forest types in all strata (R^2 0.017 to 0.050; $p = 0.001$). Environmental predictors explained 3.2 to 3.8 percent of variation in trees and shrubs and were not significant for herbs and regeneration. Trees had the highest Shannon diversity (1.391 ± 0.595), whereas herbs had the lowest (0.325 ± 0.451). For regeneration richness, random forest showed modest cross-validated performance (root mean square error 1.165 ± 0.182 ; coefficient of determination 0.142 ± 0.040).

Conclusions: Forest types impose a statistically detectable but limited macro-environmental signal across strata. Community assembly is dominated by fine-scale heterogeneity and vertical decoupling among layers, and regeneration is only weakly predictable from coarse environmental gradients. These results provide a baseline for monitoring unmanaged broadleaved forests within the sampled 260–1 964 m range.

28 **Keywords:** elevational gradient, plant community, tropical mountain forest,
29 species–environment relationships, community assembly, diversity, regeneration, ordination,
30 canonical correspondence analysis, indicator species

31 **1 Introduction**

32 Elevational gradients constitute powerful natural laboratories for understanding how climate,
33 topography, and habitat heterogeneity interact to structure plant communities. Because temper-
34 ature, moisture availability, and growing-season length vary predictably with altitude, moun-
35 tain systems have long served as test beds for ecological theory addressing species richness,
36 environmental filtering, and community turnover (Lomolino, 2001; Rahbek, 2005). Across
37 regions, richness–elevation relationships are frequently unimodal but vary with spatial extent,
38 taxonomic scope, and climatic context, indicating that no single mechanism universally governs
39 elevational diversity patterns (Grytnes and Vetaas, 2002; McCain, 2009). In forest ecosystems,
40 steep abiotic gradients combined with fine-scale variation in soils, canopy structure, and distur-
41 bance regimes generate pronounced compositional turnover and vertically stratified responses
42 among trees, shrubs, and herb layers (Gilliam, 2007; Sundqvist et al., 2013). Mountain floras
43 therefore often exhibit high beta diversity over short distances, reflecting both dispersal limita-
44 tion and niche differentiation along climatic and edaphic gradients (Qian et al., 2005). Recent
45 research has increasingly focused on disentangling the relative roles of environmental filtering,
46 functional traits, and biotic interactions in shaping elevational community organization (Siefert
47 et al., 2013; Kraft et al., 2015). Nevertheless, many studies continue to focus primarily on
48 canopy trees, despite mounting evidence that understory strata respond more sensitively to
49 microclimatic and edaphic variation and may follow distinct compositional trajectories along
50 the same gradient (Gilliam, 2007; Lenoir et al., 2008). Regeneration layers are especially infor-
51 mative in this context because they integrate recent recruitment processes and may foreshadow
52 future changes in forest composition under ongoing climatic warming (Clark et al., 2014).

53 The eastern Himalaya represents a global centre of biodiversity characterized by ex-
54 treme elevational relief, complex terrain, and monsoonal climates that generate sharp forest

55 transitions and substantial species turnover (Myers et al., 2000; Grytnes and Vetaas, 2002).
56 Within this region, numerous studies have documented steep elevational zonation and marked
57 diversity patterns, while broad-scale syntheses emphasize the region’s sharp biodiversity gra-
58 dients and habitat heterogeneity (Myers et al., 2000; Grytnes and Vetaas, 2002). Despite this
59 growing body of work, community-level investigations integrating multiple vegetation strata
60 across Himalayan elevational gradients remain comparatively uncommon. Few studies explic-
61 itly compare species–environment relationships among canopy and understorey layers, and re-
62 generation dynamics are seldom analysed in parallel with diversity and compositional patterns,
63 despite their central importance for forest resilience and long-term reorganization (Sundqvist
64 et al., 2013; Clark et al., 2014).

65 Here, we present a multi-stratum assessment of plant community composition, diversity,
66 and species–environment relationships along an elevational gradient in south-central Bhutan.
67 We test whether forest types differ in composition across four strata—trees, shrubs, herbs, and
68 regeneration—identify macro-environmental correlates of community structure, and quantify
69 elevational trends in alpha and beta diversity together with indicator species. We also use
70 machine-learning models as exploratory tools to evaluate which measured variables are asso-
71 ciated with regeneration richness. By integrating multiple vegetation strata within a unified
72 framework, this study provides one of few multi-stratum assessments in the eastern Himalaya
73 and explicitly evaluates scale mismatch between macro predictors and microsite processes.

74 **2 Methods**

75 **2.1 Study area**

76 The study was conducted in unmanaged forests of Sarpang District in south-central Bhutan un-
77 der the jurisdiction of Divisional Forest Office, Sarpang. The region spans a pronounced eleva-
78 tional gradient from approximately 153 to 3 500 m a.s.l., encompassing subtropical broadleaved
79 forests at lower elevations (100–500 m), warm broadleaved forests at mid-elevations (500–
80 1 500 m), and cool broadleaved forests between 1 500 and 3 000 m. Such steep altitudinal
81 transitions typify Himalayan landscapes and generate strong climatic and edaphic gradients

82 over short distances (Grytnes and Vetaas, 2002; Körner, 2007) (Figure 1).

83 This broader regional range provides ecological context; all statistical inference in this
84 study is based on sampled plots spanning approximately 260 to 1 964 m a.s.l.

85 Annual precipitation is high and strongly seasonal, reflecting monsoon circulation in-
86 tensified by orographic uplift, a defining feature of the eastern Himalayan foothills (Bookhagen
87 and Burbank, 2010). Rugged terrain and variable slope exposure create pronounced microcli-
88 matic heterogeneity, which is expected to contribute to high beta diversity and fine-scale com-
89 munity turnover along the gradient (Grytnes and Vetaas, 2002). The landscape also forms part
90 of a strategic ecological linkage among Bhutan's protected areas, although the sampled forests
91 themselves lie largely outside formal management regimes.

92 **2.2 Sampling design**

93 Vegetation sampling followed a stratified random design along the elevational gradient ex-
94 tending from Shershong (approximately 260 m a.s.l.) in the south to Singye (approximately
95 1 964 m a.s.l.) in the north. A total of 220 plots were established across forest types to ensure
96 representation of major vegetation zones and environmental conditions.

97 Each plot measured 20×20 m (400 m^2), a size widely used in forest community studies
98 to characterise tree assemblages and stand structure, with a nested 2×2 m subplot used to
99 survey herbaceous vegetation. Fieldwork was undertaken between March and November to
100 encompass seasonal variability in understorey communities while avoiding periods of peak
101 monsoon inaccessibility. Plots were distributed approximately evenly among elevational bands
102 and forest types to ensure balanced representation of vegetation zones. Within each band, plot
103 locations were stratified by forest type and positioned using random bearings and distances
104 from access transects, subject to terrain safety and forest accessibility constraints.

105 **2.3 Vegetation data collection**

106 All free-standing woody individuals with diameters at breast height (DBH) > 10 cm and height
107 > 1.3 m were recorded as trees. DBH was measured using diameter tapes, and total height was
108 estimated by using hypsometers. Shrubs were assessed for presence, height, and lateral spread,

109 while herbaceous species were quantified within subplots using percentage cover, frequency,
110 and maximum height.

111 Regeneration comprised all woody individuals below the canopy layer that had not yet
112 reached the tree stratum. Seedlings were defined as individuals ≤ 1.3 m in height, irrespective
113 of stem diameter, whereas saplings were defined as individuals > 1.3 m in height with DBH \leq
114 10 cm. Species exceeding 10 cm DBH were assigned to the tree layer. Regeneration richness
115 therefore integrated both seedling and sapling cohorts, representing early demographic stages
116 that are particularly sensitive to microsite conditions and neighborhood effects.

117 Species identifications were verified using regional floras and herbarium reference ma-
118 terial, and taxonomic nomenclature was cross-checked against the World Flora Online database
119 (accessed 6 Feb 2026). Structural attributes, including basal area, DBH-class distributions, and
120 height-class distributions, were derived to characterize stand structure and regeneration dynam-
121 ics across forest types and elevational gradients.

122 **2.4 Environmental variables**

123 Topographic attributes (latitude and longitude), including elevation, slope, and aspect, were
124 recorded in the field using handheld Global Positioning System receivers, clinometers, and
125 compasses. Spatial climatic surfaces describing air temperature, precipitation, evapotranspi-
126 ration, and water balance were extracted from the national gridded climate dataset produced
127 by Dorji et al. (2025), developed by CSIRO and distributed with a permanent digital object
128 identifier (<https://doi.org/10.25919/pec2-hs50>).

129 Environmental values were extracted at plot coordinates using the dataset's native grid
130 and historical baseline layers (1986–2015), consistent with the metadata provided for the
131 archived climate product.

132 These climate layers were used consistently across all spatial and statistical analyses.

133 **2.5 Data preparation**

134 Field records were curated in tabular format to compute species abundance, frequency, basal
135 area and importance value index separately for each vegetation stratum. Alpha diversity was

136 quantified using the Shannon–Wiener index (H'), Simpson’s diversity index ($1 - D$) and
137 Pielou’s evenness (J) for each forest type and vegetation layer (Shannon, 1948; Simpson,
138 1949; Pielou, 1966).

139 **2.6 Multivariate community analyses**

140 Floristic variation among plots was examined using non-metric multidimensional scaling
141 (NMDS) based on Bray–Curtis dissimilarities (Bray and Curtis, 1957; Kruskal, 1964).
142 Species–environment relationships were assessed using canonical correspondence analysis
143 (CCA), which constrains ordination axes by linear combinations of climatic and topographic
144 predictors (ter Braak, 1986). Ordination axes were interpreted through correlations between
145 site scores and environmental variables.

146 Community differences among forest types were tested using permutational multivari-
147 ate analysis of variance (Anderson, 2001). NMDS was computed with two dimensions ($k = 2$)
148 and a fixed random seed (42) to ensure reproducibility. Environmental vectors were fitted using
149 permutation tests with 999 randomizations. PERMANOVA was conducted with 999 permuta-
150 tions, and homogeneity of multivariate dispersions was evaluated using permutation tests on
151 distance-to-centroid values (Warton et al., 2012).

152 To support valid interpretation, PERMANOVA results were interpreted jointly with ef-
153 fect sizes (R^2) and dispersion tests. In strata with heterogeneous dispersion, PERMANOVA was
154 interpreted as reflecting combined centroid and spread effects rather than pure location shifts
155 (Warton et al., 2012). NMDS was used for pattern visualization rather than as a stand-alone
156 test of group separation.

157 Prior to CCA, collinearity among predictors was assessed using variance inflation fac-
158 tors, and variables exceeding a threshold of 10 were sequentially removed following determin-
159 istic selection rules. Statistical significance of constrained axes and individual predictors was
160 evaluated using 999 permutations.

161 Indicator species analysis was applied to identify taxa significantly associated with for-
162 est types using the indicator value method, with significance assessed at $\alpha = 0.05$ and 999
163 permutations (Dufrêne and Legendre, 1997).

164 **2.7 Regeneration dynamics and predictive modelling**

165 Seedling and sapling data were analysed to quantify regeneration patterns and spatial structure
166 across forest types and elevations. Environmental drivers of regeneration richness were mod-
167 elled using random forest and extreme gradient boosting algorithms, both of which are widely
168 applied for non-linear ecological prediction problems (Breiman, 2001; Chen and Guestrin,
169 2016). Random forest models were fitted with 500 trees, and predictor importance was quanti-
170 fied as the percentage increase in mean squared error following permutation. Gradient boosting
171 models were parameterized with 100 boosting rounds, a maximum tree depth of four and a
172 learning rate of 0.1, and predictor influence was assessed using relative gain values.

173 Model performance was evaluated using five-fold cross-validation with a fixed random
174 seed (42) to ensure reproducibility. Predictive accuracy was summarized using cross-validated
175 error statistics and explained variance, and response curves were inspected to verify ecolog-
176 ically plausible relationships between regeneration patterns and key climatic or topographic
177 predictors.

178 Because predictive performance was modest, variable-importance results were inter-
179 preted as exploratory indicators of potential drivers rather than definitive causal rankings.

180 **2.8 Software environment**

181 All analyses were conducted in R. Community-ecology workflows, including ordination,
182 dissimilarity-based testing and indicator-species analysis, were implemented primarily using
183 functions described in the ecological literature underlying widely adopted multivariate
184 methods (ter Braak, 1986; Anderson, 2001; Duf r ne and Legendre, 1997). Results from
185 selected multivariate classifications and indicator-species procedures were independently
186 verified in PC-ORD version 5 to confirm analytical consistency. Microsoft Excel was used for
187 preliminary data curation and quality-control screening prior to statistical analysis.

188 **2.9 Reproducibility and data stewardship**

189 Reproducibility was ensured through systematic archiving of raw field observations, spatial en-
190 vironmental layers, curated analysis tables and derived outputs. All distance measures, ordina-
191 tion settings, permutation schemes and machine-learning hyperparameters were documented in
192 metadata files accompanying the archived datasets. Intermediate products, including ordination
193 scores, regeneration prediction surfaces, cross-validation partitions and variable-importance ta-
194 bles were retained to permit independent replication of all analytical steps.

195 Upon submission, data and code supporting the results will be deposited in a public
196 repository with a digital object identifier in accordance with data-sharing policy, with
197 anonymized access provided during double-blind peer review.

198 **3 Results**

199 **3.1 Community composition and ordination**

200 Non-metric multidimensional scaling (NMDS) showed modest but detectable compositional
201 differentiation among forest types across strata (Figure 2). Stress values were uniformly low
202 (trees = 0.0001; shrubs = 0.070; herbs = 0.001; regeneration = 0.0006), indicating a low-stress
203 two-dimensional rank-order fit of Bray–Curtis dissimilarities rather than a perfect ordination
204 (Appendix S3). We explored multiple dimensional solutions, and stress values remained con-
205 sistently low, confirming ordination stability.

206 The near-zero stress values for trees, herbs, and regeneration likely arise from matrix
207 properties that ease low-dimensional rank fitting (for example, high tied dissimilarities and
208 sparse compositional structure), so ordinations were interpreted conservatively as broad sum-
209 maries rather than precise geometric distances (Kruskal, 1964; Clarke, 1993). We therefore
210 cross-checked NMDS patterns against PERMANOVA, dispersion tests, and constrained ordi-
211 nation instead of relying on visual separation alone.

212 Shrub and herb assemblages displayed the greatest dispersion in ordination space and
213 the strongest alignment with fitted climatic vectors, particularly temperature, evapotranspira-

214 tion and precipitation (Figure 2B–C). Tree assemblages were comparatively compressed along
215 NMDS axes (Figure 2A), while regeneration plots showed broad scatter (Figure 2D), together
216 indicating vertical decoupling and strong neighbourhood-scale heterogeneity.

217 These stratified responses mirror documented altitudinal forest-type transitions along
218 Bhutanese dry valley slopes (Wangda and Ohsawa, 2006a).

219 **3.2 Community differences among forest types**

220 Community composition differed significantly among forest types across all vegetation strata
221 (Table 1). Tree assemblages exhibited modest but statistically significant separation (PER-
222 MANOVA $R^2 = 0.031$, $F = 3.38$, $p = 0.001$), with homogeneous dispersions (betadisper $p =$
223 0.291), indicating that group differences reflected centroid shifts rather than unequal within-
224 group variability (Appendix S2).

225 Shrub communities showed the strongest differentiation among forest types
226 ($R^2 = 0.050$, $F = 5.05$, $p = 0.001$), although dispersions were heterogeneous ($p = 0.001$),
227 suggesting that both location and spread contributed to observed differences. Herb and
228 regeneration assemblages also differed significantly ($R^2 = 0.017$ and 0.021 , respectively; both
229 $p = 0.001$), but only the herb stratum showed heterogeneous dispersion (Table 1).

230 The greater sensitivity of shrub and herb layers relative to trees is consistent with
231 reported altitudinal zonation and vegetation transitions in Himalayan forests (Wangda and
232 Ohsawa, 2006a; Grierson and Long, 2001). In strata with heterogeneous dispersion, PER-
233 MANOVA reflects combined centroid and spread effects. Accordingly, shrub and herb results
234 were interpreted as mixed location–dispersion signals, whereas homogeneous dispersions for
235 trees and regeneration indicate that their compositional differences more closely represent cen-
236 troid shifts.

237 **3.3 Species–environment relationships**

238 Canonical correspondence analysis revealed that selected environmental variables—aspect,
239 evapotranspiration, latitude, longitude and slope—explained a small but statistically significant
240 fraction of constrained inertia in trees and shrubs. The percentage of total inertia explained

241 was 3.2% for trees ($p = 0.008$) and 3.8% for shrubs ($p = 0.001$; Table 2; Figure 5). For herbs
242 and regeneration, constrained models explained 3.4% of total inertia but were not significant at
243 $\alpha = 0.05$ ($p = 0.125$ and 0.076 , respectively) (Appendix S9).

244 CCA biplots illustrated contrasting environmental associations among strata (Figure 5).
245 Tree communities aligned primarily with slope and aspect gradients, shrub assemblages were
246 most strongly oriented toward evapotranspiration and latitudinal position, while herbaceous
247 vegetation responded to combined slope–climate axes. Regeneration patterns were weakly
248 associated with evapotranspiration and aspect.

249 The low proportion of constrained inertia across all strata is expected in steep, hetero-
250 geneous Himalayan terrain and is consistent with substantial unmeasured microsite drivers op-
251 erating within broader altitudinal transitions (Grytnes and Vetaas, 2002; Wangda and Ohsawa,
252 2006a).

253 **3.4 Diversity patterns**

254 Alpha diversity differed markedly among vegetation strata (Table 3; Figure 3). Trees exhibited
255 the highest mean species richness (5.30 ± 2.57 species per plot) and Shannon diversity ($1.391 \pm$
256 0.595), followed by shrubs (richness = 4.77 ± 3.43 ; Shannon = 1.063 ± 0.706), regeneration
257 (richness = 2.00 ± 1.26 ; Shannon = 0.443 ± 0.499) and herbs (richness = 1.79 ± 1.32 ; Shannon
258 = 0.325 ± 0.451). Pielou's evenness was highest for trees (0.903) and lowest for herbs (0.804).

259 Species accumulation curves approached asymptotes most rapidly for shrubs and regen-
260 eration, whereas trees and herbs continued to increase steadily with sampling effort, indicating
261 incomplete saturation of the regional species pool in these strata (Figure 4). Such patterns are
262 consistent with documented altitudinal zonation of Bhutanese dry-valley forests and reported
263 regeneration dynamics of dominant trees (Wangda and Ohsawa, 2006a,b). Continued species
264 accumulation in tree and herb strata suggests that additional sampling would likely yield further
265 taxa, particularly rare canopy species and ephemeral understorey herbs, indicating substantial
266 compositional turnover.

267 Species richness varied along the elevational gradient for all strata (Figure 7). Shrubs
268 displayed a unimodal mid-elevation peak, whereas trees showed comparatively stable richness

269 across the sampled range, and herbs and regeneration exhibited weaker, irregular trends. These
270 responses align with Himalayan studies reporting mid-elevation richness peaks and altitudi-
271 nal zonation in woody layers (Acharya et al., 2011; Grytnes and Vetaas, 2002; Wangda and
272 Ohsawa, 2006a).

273 Beta diversity (Whittaker's β) was highest for herbs (75.04), followed by regeneration
274 (54.63), trees (41.86) and shrubs (23.89), indicating pronounced species turnover in the herb
275 layer relative to the regional species pool.

276 **3.5 Indicator species**

277 Indicator-species analysis detected significant associations with elevational classes across all
278 strata (Table 4). Shrubs contained the largest proportion of indicator taxa (15 of 101 species;
279 14.9%), followed by herbs (10 of 134; 7.5%), regeneration (8 of 109; 7.3%) and trees (10 of
280 221; 4.5%) (Appendix S4).

281 Among canopy trees, *Schima wallichii* and *Castanopsis indica* were characteristic of
282 low- to mid-elevation forests, whereas *Alnus nepalensis* was associated with higher elevations.
283 These patterns accord with floristic zonation documented in Bhutanese mountain forests, where
284 evergreen broadleaved species dominate lower belts and pioneer or cool-adapted taxa become
285 more frequent upslope (Wangda and Ohsawa, 2006a; Grierson and Long, 2001).

286 **3.6 Regeneration modelling**

287 Random forest produced modest predictive performance for regeneration richness (Table 5;
288 Figure 6), with cross-validated $R^2 = 0.142 \pm 0.040$ and RMSE 1.165 ± 0.182 . Gradient boost-
289 ing showed near-zero to negative explanatory power ($R^2 = -0.009 \pm 0.096$; RMSE = $1.261 \pm$
290 0.192) (Appendix S5).

291 Fold-level diagnostics (Appendix S7) showed moderate variability in RF performance
292 (R^2 range: 0.096–0.193; RMSE range: 0.999–1.476) and unstable XGBoost performance (R^2
293 range: -0.154 to 0.106; RMSE range: 1.102–1.570), reinforcing that coarse predictors provide
294 only weak predictability of recruitment.

295 Variable-importance rankings indicated that shrub-layer attributes, together with tem-
296 perature, elevation and evapotranspiration, were the strongest correlates of regeneration rich-
297 ness (Figure 6; Appendix S6). Ecologically, this pattern is consistent with neighbourhood-scale
298 filtering and local biotic interactions outweighing coarse macro-environmental gradients for
299 early life stages (Wangda and Ohsawa, 2006b).

300 Given the low explanatory power, these models are interpreted as exploratory ecological
301 inference rather than deterministic prediction. Important drivers—such as canopy openness,
302 disturbance history, soil properties or fine-scale moisture regimes—were not fully captured
303 by the available predictors, a common limitation in forest-regeneration modelling in complex
304 mountain terrain (Elith et al., 2008).

305 **4 Discussion**

306 **4.1 Stratified community turnover along elevational gradients**

307 Our analyses indicate clear vertical stratification in community turnover, with understorey as-
308 semblages (shrubs and herbs) more variable than canopy trees. This pattern mirrors observa-
309 tions from other Himalayan forests where understorey communities respond strongly to micro-
310 climatic and edaphic heterogeneity, whereas long-lived canopy trees integrate conditions over
311 broader temporal and spatial scales (Wangda and Ohsawa, 2006a; Grytnes and Vetaas, 2002).
312 Forest-type effects were statistically detectable but limited in magnitude: PERMANOVA ex-
313 plained only 1.7–5.0% of compositional variation ($R^2 = 0.017\text{--}0.050$, $p = 0.001$). These low
314 effect sizes are compatible with high beta diversity and fine-grained heterogeneity in montane
315 systems (Acharya et al., 2011; Carpenter, 2005). Importantly, interpretation depends on dis-
316 persion structure: in shrub and herb strata, heterogeneous dispersions indicate mixed location-
317 spread effects, whereas tree and regeneration strata with homogeneous dispersions indicate
318 clearer centroid shifts among forest types. This cross-stratum contrast supports vertical de-
319 coupling, where canopy differentiation is detectable but modest and understorey turnover is
320 dominated by neighbourhood-scale heterogeneity.

321 **4.2 Environmental drivers and scale of control**

322 Direct gradient analyses (CCA) showed that aspect, slope, evapotranspiration, and spatial po-
323 sition explained only a small fraction of floristic variation ($\approx 3\text{--}4\%$ in trees and shrubs). Rather
324 than indicating weak study design, this low constrained inertia is expected in steep Himalayan
325 terrain, where microtopography, canopy gaps, soils, and disturbance history vary at much finer
326 scales than gridded macro predictors (Grytnes and Vetaas, 2002; Wangda and Ohsawa, 2006a).
327 The contrasting orientations among strata reinforce this scale mismatch. Tree communities
328 aligned mainly with slope and aspect, while shrubs and regeneration were more associated
329 with evapotranspiration and latitude; herbs tracked mixed slope–climate axes. Together, these
330 patterns indicate that macro-environmental gradients are detectable but limited, and that com-
331 munity assembly is dominated by microsite processes and vertical decoupling among strata.

332 **4.3 Diversity patterns and beta-diversity**

333 Marked differences in alpha diversity among strata further highlight the vertically structured
334 nature of Himalayan broadleaved forests. Tree layers in our study maintained high species
335 richness and evenness across the gradient, reflecting the coexistence of multiple canopy domi-
336 nants in these unmanaged stands – a feature repeatedly documented in Bhutan’s warm and cool
337 broadleaved forests (Grierson and Long, 2001; Wangda and Ohsawa, 2006a). Shrub richness
338 peaked at mid-elevations, consistent with many Himalayan studies that find unimodal diversity
339 curves in the woody understorey around intermediate altitudes where moisture, temperature,
340 and structural complexity are jointly optimized (Grytnes and Vetaas, 2002). By contrast, herbs
341 and regeneration showed weak or irregular elevational trends in richness, coupled with elevated
342 beta diversity relative to alpha diversity in the herb layer. This pattern implies that small-scale
343 environmental mosaics, rather than smooth elevational forcing, structure ground-layer com-
344 munities. High herb-layer beta diversity is widely reported in Himalayan forests and alpine
345 systems, where aspect, litter depth, and gap dynamics generate sharp species turnover over
346 short distances (Grytnes and Vetaas, 2002). The fact that our species accumulation curves did
347 not fully asymptote for trees and herbs even after 221 plots suggests that a considerable portion
348 of the regional species pool remained unsampled in these strata, consistent with substantial

349 compositional turnover.

350 **4.4 Indicator species and floristic transitions**

351 Indicator species analysis revealed fewer significant canopy indicators than shrub and herb in-
352 dicators, supporting vertical decoupling in habitat filtering strength. Low tree indicator speci-
353 ficity is consistent with broader niche amplitudes in canopy taxa across the sampled gradient.
354 In contrast, stronger shrub and herb differentiation implies finer-scale filtering in understorey
355 microsites. This contrast aligns with Himalayan zonation as overlapping distributions rather
356 than discrete boundaries (Ohsawa, 1995; Wangda and Ohsawa, 2006a).

357 **4.5 Regeneration dynamics and model interpretation**

358 Machine-learning results were used as exploratory ecological evidence on regeneration con-
359 trols. The best model (random forest) explained only about 14% of cross-validated variance
360 ($R^2 \approx 0.14$), indicating weak predictability from the available coarse predictors. Shrub-layer
361 structure emerged as the strongest correlate, supporting neighbourhood-scale filtering during
362 early recruitment. This interpretation is consistent with Bhutanese forest observations that lo-
363 cal stand structure influences regeneration (Wangda and Ohsawa, 2006a,b). The low predictive
364 power also indicates missing microsite drivers, such as canopy openness, soil properties, distur-
365 bance history, and fine-scale moisture (Elith et al., 2008). Accordingly, these models should not
366 be read as deterministic forecasts, but as evidence that regeneration is only weakly predictable
367 from macro-environmental gradients in this landscape.

368 **4.6 Limitations and novelty of the study**

369 Several caveats merit consideration. First, climate variables were derived from interpolated sur-
370 faces (Dorji et al., 2025) and may not capture plot-level microclimate in steep terrain. Second,
371 heterogeneous dispersion in shrub and herb strata means that part of PERMANOVA signifi-
372 cance reflects spread differences, not only centroid shifts. Third, regeneration measurements
373 represent a temporal snapshot and may miss episodic establishment dynamics of slow-growing

374 montane trees. Spatial autocorrelation was not explicitly modeled, which may influence fine-
375 scale inference, and future work could apply spatially explicit approaches. Even with these con-
376 straints, this study provides one of few multi-stratum assessments in the eastern Himalaya. The
377 main contribution is to show that broad-scale environmental effects are statistically detectable
378 but limited, while fine-scale heterogeneity, neighbourhood filtering, and vertical decoupling
379 dominate assembly patterns.

380 **5 Conclusions**

381 Across 260–1964 m a.s.l. in south-central Bhutan, forest types imposed a statistically
382 detectable but limited macro-environmental signal on community composition ($R^2 = 0.017$ –
383 0.050). Understorey strata showed greater turnover and higher dispersion than canopy trees,
384 indicating strong vertical stratification and decoupling among layers.

385 CCA explained only about 3–4% of variation, which is consistent with steep
386 Himalayan terrain where microsite heterogeneity is high and many local drivers are
387 unmeasured. PERMANOVA interpretation was therefore conditioned on dispersion structure,
388 with mixed centroid–spread effects in heterogeneous strata.

389 Regeneration was only weakly predictable from coarse predictors (random forest CV
390 $R^2 \approx 0.14$), and shrub-layer attributes emerged as the strongest correlates. This supports
391 neighbourhood-scale filtering during early recruitment and reinforces that macro gradients
392 alone do not capture regeneration dynamics.

393 This study provides a baseline for long-term monitoring of unmanaged broadleaved
394 forests in the sampled elevation range. Inference should remain restricted to this 260–1964 m
395 gradient.

396 **References**

397 Acharya, B. K., B. Chettri, and L. Vijayan (2011). Distribution pattern of trees along an eleva-
398 tional gradient of Eastern Himalaya, India. *Acta Oecologica* 37, 329–336.

- 399 Anderson, M. J. (2001). A new method for non-parametric multivariate analysis of variance.
400 *Austral Ecology* 26, 32–46.
- 401 Bookhagen, B. and D. W. Burbank (2010). Toward a complete Himalayan hydrological budget:
402 Spatiotemporal distribution of snowmelt and rainfall and their impact on river discharge.
403 *Journal of Geophysical Research: Earth Surface* 115, F03019.
- 404 Bray, J. R. and J. T. Curtis (1957). An ordination of the upland forest communities of southern
405 Wisconsin. *Ecological Monographs* 27, 325–349.
- 406 Breiman, L. (2001). Random forests. *Machine Learning* 45, 5–32.
- 407 Carpenter, C. (2005). The environmental control of plant species density on a Himalayan
408 elevation gradient. *Journal of Biogeography* 32, 999–1018.
- 409 Chen, T. and C. Guestrin (2016). XGBoost: A scalable tree boosting system. In *Proceedings*
410 *of the 22nd ACM SIGKDD International Conference on Knowledge Discovery and Data*
411 *Mining*, pp. 785–794.
- 412 Clark, J. S., D. Bell, C. Chu, B. Courbaud, M. Dietze, M. Hersh, et al. (2014). High-
413 dimensional coexistence based on individual variation: A synthesis of evidence. *Ecological*
414 *Monographs* 84, 3–42.
- 415 Clarke, K. R. (1993). Non-parametric multivariate analyses of changes in community structure.
416 *Australian Journal of Ecology* 18, 117–143.
- 417 Dorji, T. et al. (2025). Bhutan high-resolution climate surfaces (historical 1986–2015 and future
418 2015–2100). CSIRO Data Collection.
- 419 Dufrière, M. and P. Legendre (1997). Species assemblages and indicator species: The need for
420 a flexible asymmetrical approach. *Ecological Monographs* 67, 345–366.
- 421 Elith, J., J. R. Leathwick, and T. Hastie (2008). A working guide to boosted regression trees.
422 *Journal of Animal Ecology* 77, 802–813.

- 423 Gilliam, F. S. (2007). The ecological significance of the herbaceous layer in temperate forest
424 ecosystems. *BioScience* 57, 845–858.
- 425 Grierson, A. J. C. and D. G. Long (1983–2001). *Flora of Bhutan*. Edinburgh, UK: Royal
426 Botanical Garden Edinburgh and Royal Government of Bhutan.
- 427 Grytnes, J.-A. and O. R. Vetaas (2002). Species richness and altitude: A comparison between
428 null models and interpolated plant species richness along the Himalayan altitudinal gradient,
429 Nepal. *The American Naturalist* 159, 294–304.
- 430 Körner, C. (2007). The use of ‘altitude’ in ecological research. *Trends in Ecology and Evolu-*
431 *tion* 22, 569–574.
- 432 Kraft, N. J. B., O. Godoy, and J. M. Levine (2015). Plant functional traits and the multidimen-
433 sional nature of species coexistence. *Proceedings of the National Academy of Sciences of*
434 *the United States of America* 112, 797–802.
- 435 Kruskal, J. B. (1964). Nonmetric multidimensional scaling: A numerical method. *Psychome-*
436 *trika* 29, 115–129.
- 437 Lenoir, J., J.-C. Gégout, P. A. Marquet, P. de Ruffray, and H. Brisse (2008). A significant
438 upward shift in plant species optimum elevation during the twentieth century. *Science* 320,
439 1768–1771.
- 440 Lomolino, M. V. (2001). Elevation gradients of species density: Historical and prospective
441 views. *Global Ecology and Biogeography* 10, 3–13.
- 442 McCain, C. M. (2009). Global analysis of bird elevational diversity. *Global Ecology and*
443 *Biogeography* 18, 346–360.
- 444 Myers, N., R. A. Mittermeier, C. G. Mittermeier, G. A. B. da Fonseca, and J. Kent (2000).
445 Biodiversity hotspots for conservation priorities. *Nature* 403, 853–858.
- 446 Ohsawa, M. (1995). Latitudinal pattern of mountain vegetation zonation in eastern Asia and its
447 relation to climate. *Vegetatio* 121, 3–10.

- 448 Pielou, E. C. (1966). The measurement of diversity in different types of biological collections.
449 *Journal of Theoretical Biology* 13, 131–144.
- 450 Qian, H., R. E. Ricklefs, and P. S. White (2005). Beta diversity of angiosperms in temperate
451 floras of eastern Asia and eastern North America. *Ecology Letters* 8, 15–22.
- 452 Rahbek, C. (2005). The role of spatial scale and the perception of large-scale species-richness
453 patterns. *Ecology Letters* 8, 224–239.
- 454 Shannon, C. E. (1948). A mathematical theory of communication. *Bell System Technical*
455 *Journal* 27, 379–423.
- 456 Siefert, A., C. Ravenscroft, M. D. Weiser, and E. E. Cleland (2013). Functional beta-diversity
457 patterns reveal deterministic community assembly processes in eastern North American
458 trees. *Global Ecology and Biogeography* 22, 682–691.
- 459 Simpson, E. H. (1949). Measurement of diversity. *Nature* 163, 688.
- 460 Sundqvist, M. K., N. J. Sanders, and D. A. Wardle (2013). Community and ecosystem re-
461 sponses to elevational gradients. *Annual Review of Ecology, Evolution, and Systematics* 44,
462 261–280.
- 463 ter Braak, C. J. F. (1986). Canonical correspondence analysis: A new eigenvector technique
464 for multivariate direct gradient analysis. *Ecology* 67, 1167–1179.
- 465 Wangda, P. and M. Ohsawa (2006a). Gradational forest change along the climatically dry valley
466 slopes of Bhutan in the midst of humid eastern Himalaya. *Plant Ecology* 186, 109–128.
- 467 Wangda, P. and M. Ohsawa (2006b). Structure and regeneration dynamics of dominant tree
468 species along an altitudinal gradient in dry valley slopes of the Bhutan Himalaya. *Forest*
469 *Ecology and Management* 230, 136–150.
- 470 Warton, D. I., T. W. Wright, and Y. Wang (2012). Distance-based multivariate analyses con-
471 found location and dispersion effects. *Methods in Ecology and Evolution* 3, 89–101.

Table 1: Results of permutational multivariate analysis of variance (PERMANOVA) and tests of multivariate dispersion for vegetation strata across forest types. p -values are based on 999 permutations.

Stratum	Sites	Groups	R^2	F	p	Disp. F	Disp. p	Homogeneous
Trees	216	3	0.031	3.38	0.001	1.24	0.291	Yes
Shrubs	194	3	0.050	5.05	0.001	12.93	0.001	No
Herbs	206	3	0.017	1.70	0.001	15.05	0.001	No
Regeneration	205	3	0.021	2.14	0.001	1.17	0.319	Yes

Table 2: Summary of canonical correspondence analyses by vegetation stratum. Environmental variables were selected following iterative variance inflation factor screening (threshold = 10). Significance of constrained inertia was assessed using 999 permutations.

Stratum	Sites	Species	Env. vars	Total inertia	Constrained	% Explained	p
Trees	216	221	5	35.117	1.109	3.2	0.008
Shrubs	194	101	5	27.832	1.045	3.8	0.001
Herbs	206	134	5	68.475	2.309	3.4	0.125
Regeneration	205	109	5	58.906	1.987	3.4	0.076

Table 3: Mean alpha-diversity metrics by vegetation stratum. Values are mean \pm standard deviation.

Stratum	Plots	Richness	Shannon	Simpson	Evenness
Trees	221	5.30 \pm 2.57	1.391 \pm 0.595	0.665	0.903
Shrubs	198	4.77 \pm 3.43	1.063 \pm 0.706	0.524	0.832
Regeneration	209	2.00 \pm 1.26	0.443 \pm 0.499	0.264	0.839
Herbs	210	1.79 \pm 1.32	0.325 \pm 0.451	0.193	0.804

Table 4: Summary of indicator-species analysis by stratum. Groups were defined by elevational class (low, mid and high). Significance was assessed using 999 permutations at $\alpha = 0.05$.

Stratum	Sites	Species	Groups	Significant indicators	% Significant
Trees	216	221	3	10	4.5
Shrubs	194	101	3	15	14.9
Herbs	206	134	3	10	7.5
Regeneration	205	109	3	8	7.3

Table 5: Cross-validated performance of machine-learning models predicting regeneration richness across five folds. R^2 denotes coefficient of determination; RMSE, root mean square error; MAE, mean absolute error. Full fold-level output is provided in Appendix S7.

Model	Predictors	Obs.	CV R^2	CV RMSE	CV MAE
Random Forest	13	192	0.142 ± 0.040	1.165 ± 0.182	0.907
XGBoost	13	192	-0.009 ± 0.096	1.261 ± 0.192	0.942

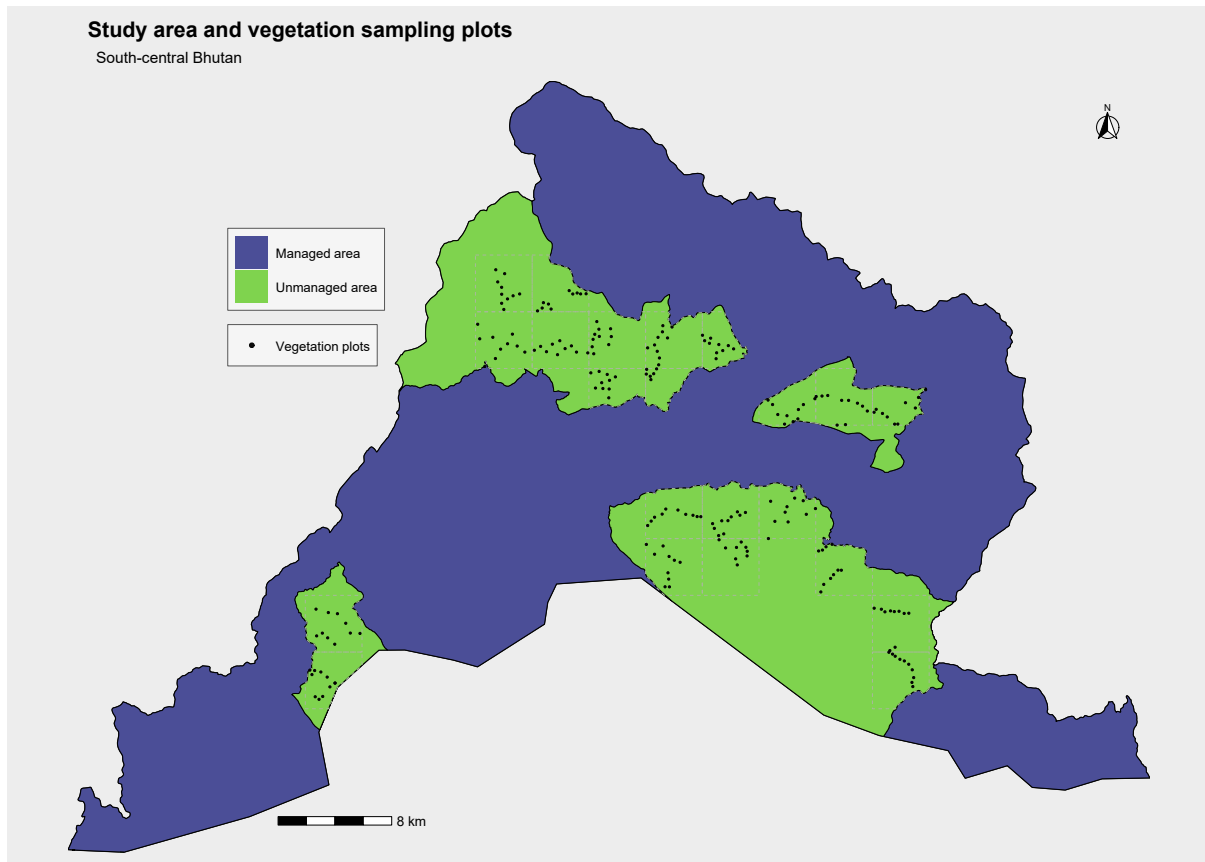


Figure 1: Study area and vegetation sampling plots in south-central Bhutan (Sarpang District). Green polygons indicate unmanaged forest areas and black points represent sampled vegetation plots along the elevational gradient.

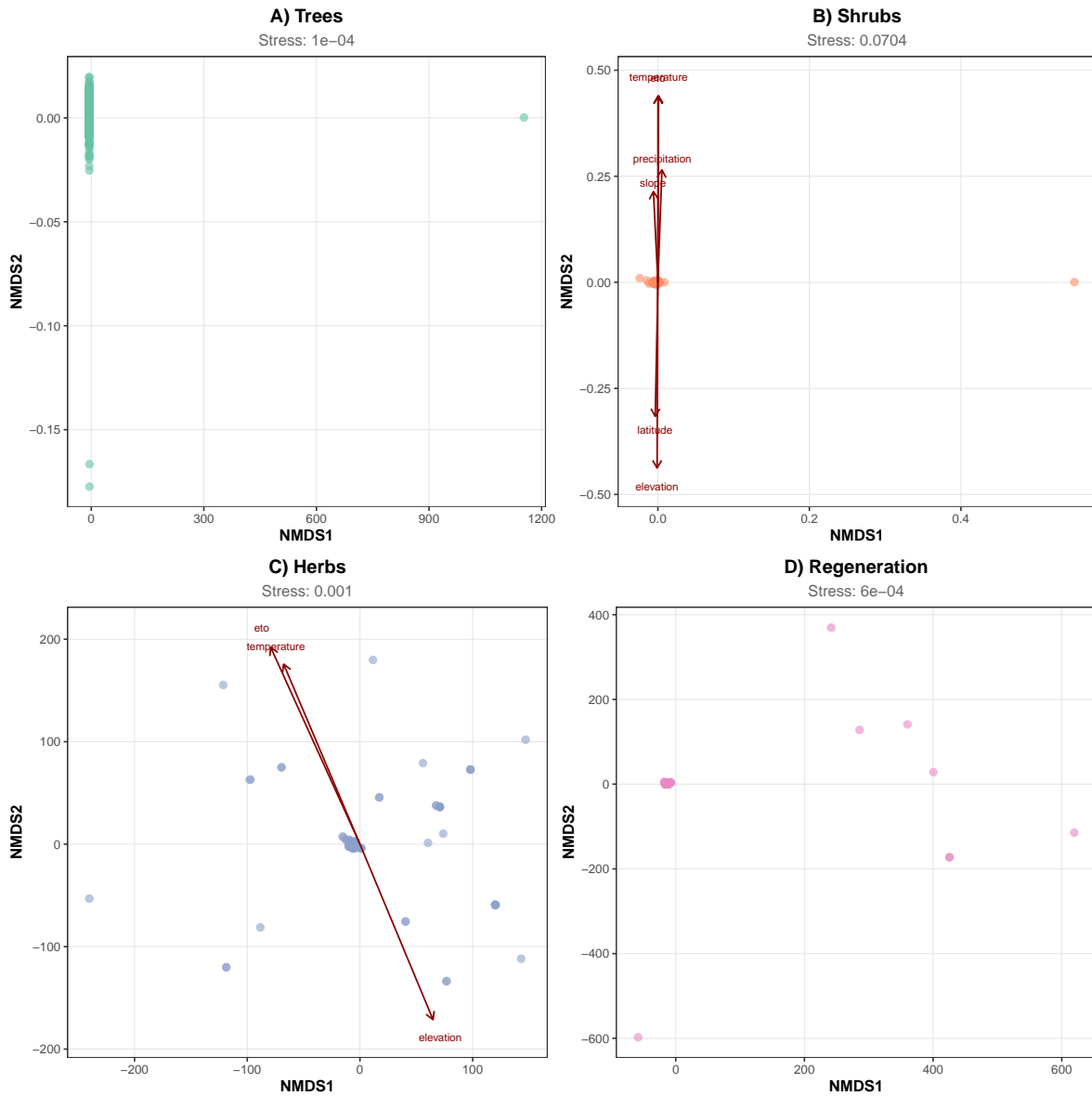


Figure 2: Non-metric multidimensional scaling (NMDS) ordinations of vegetation plots for four strata: (A) trees, (B) shrubs, (C) herbs and (D) regeneration. Points represent sample plots coloured by forest type; polygons delineate convex hulls for each forest type. Red arrows indicate fitted environmental vectors significant at $p < 0.05$ based on 999 permutations. Stress values are shown for each ordination.

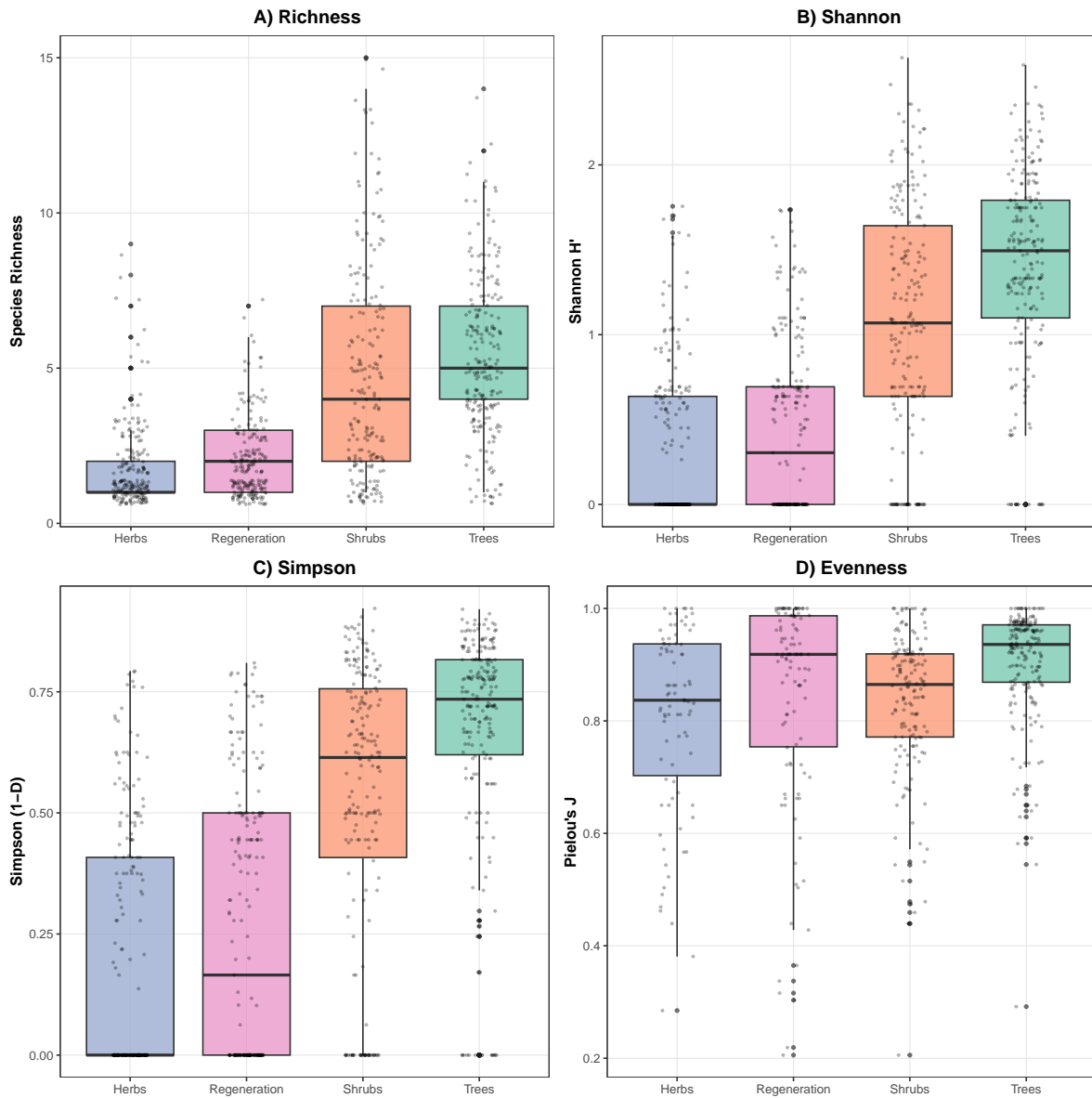


Figure 3: Alpha-diversity metrics across vegetation strata. Panels show (A) species richness, (B) Shannon diversity (H'), (C) Simpson diversity ($1 - D$) and (D) Pielou's evenness (J). Box-plots depict medians and interquartile ranges; points represent individual plots.

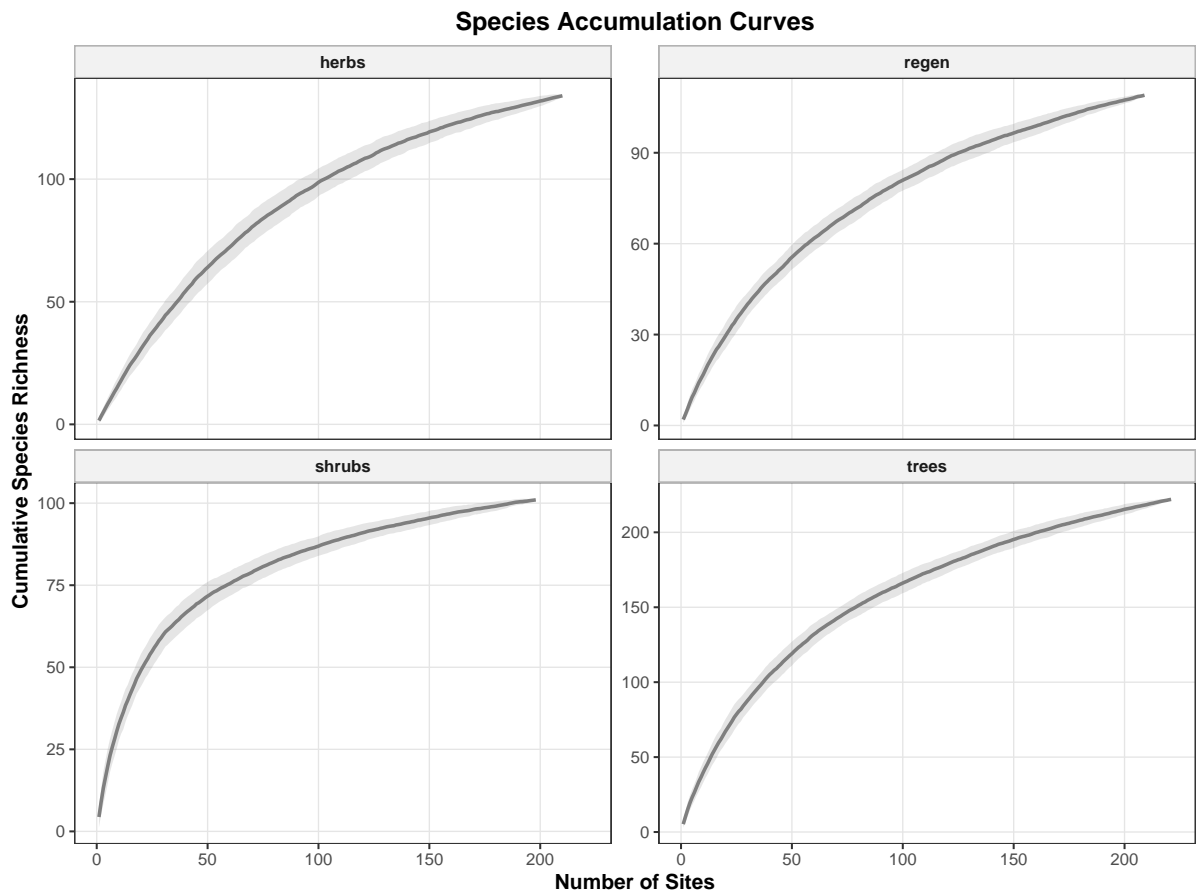


Figure 4: Sample-based species accumulation curves for herbs, regeneration, shrubs and trees. Solid lines indicate mean richness across random permutations; shaded envelopes show 95% confidence intervals.

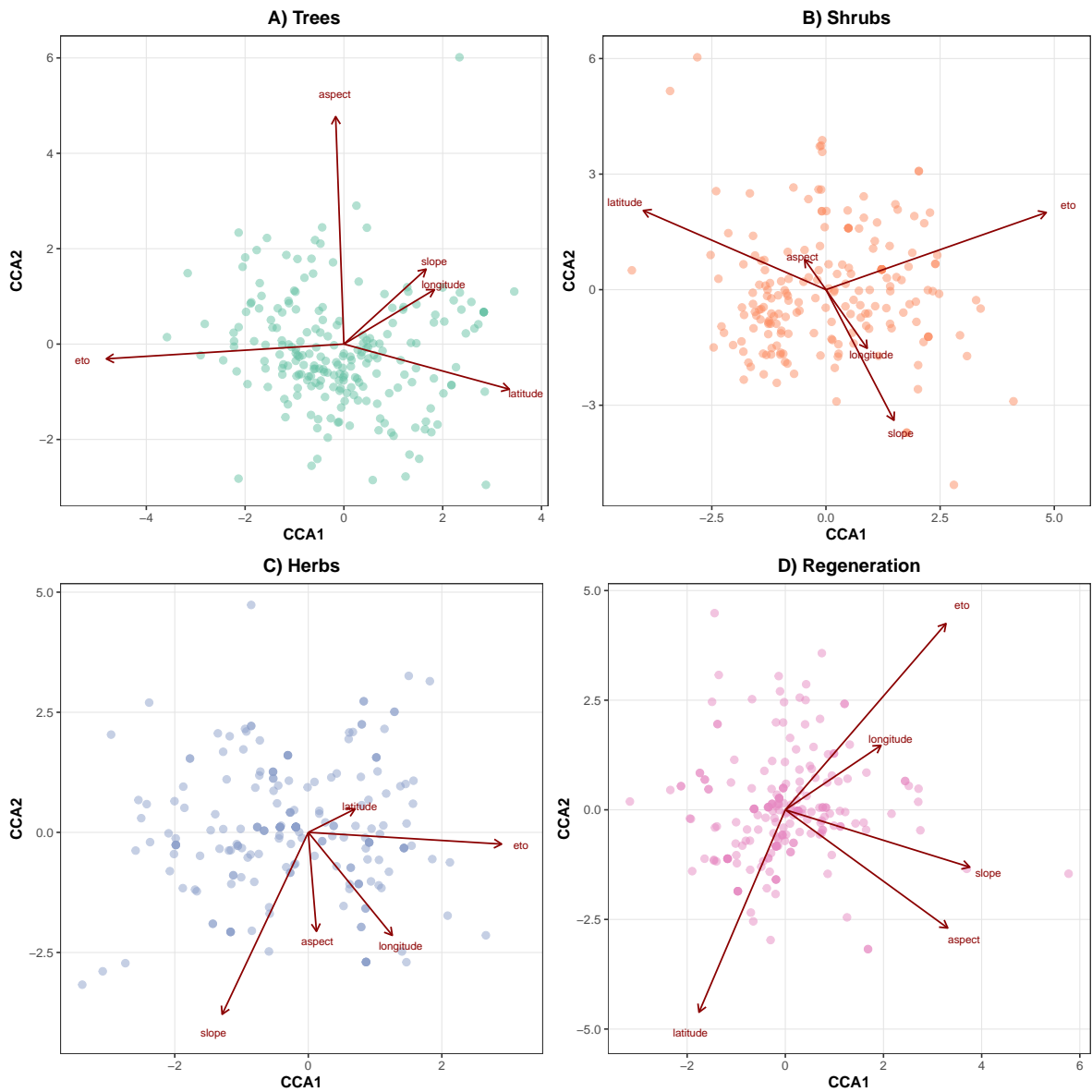


Figure 5: Canonical correspondence analysis (CCA) biplots for (A) trees, (B) shrubs, (C) herbs and (D) regeneration. Points represent plots and arrows denote environmental predictors retained after variance inflation factor screening (threshold = 10). Arrow length indicates the strength of correlations with ordination axes.

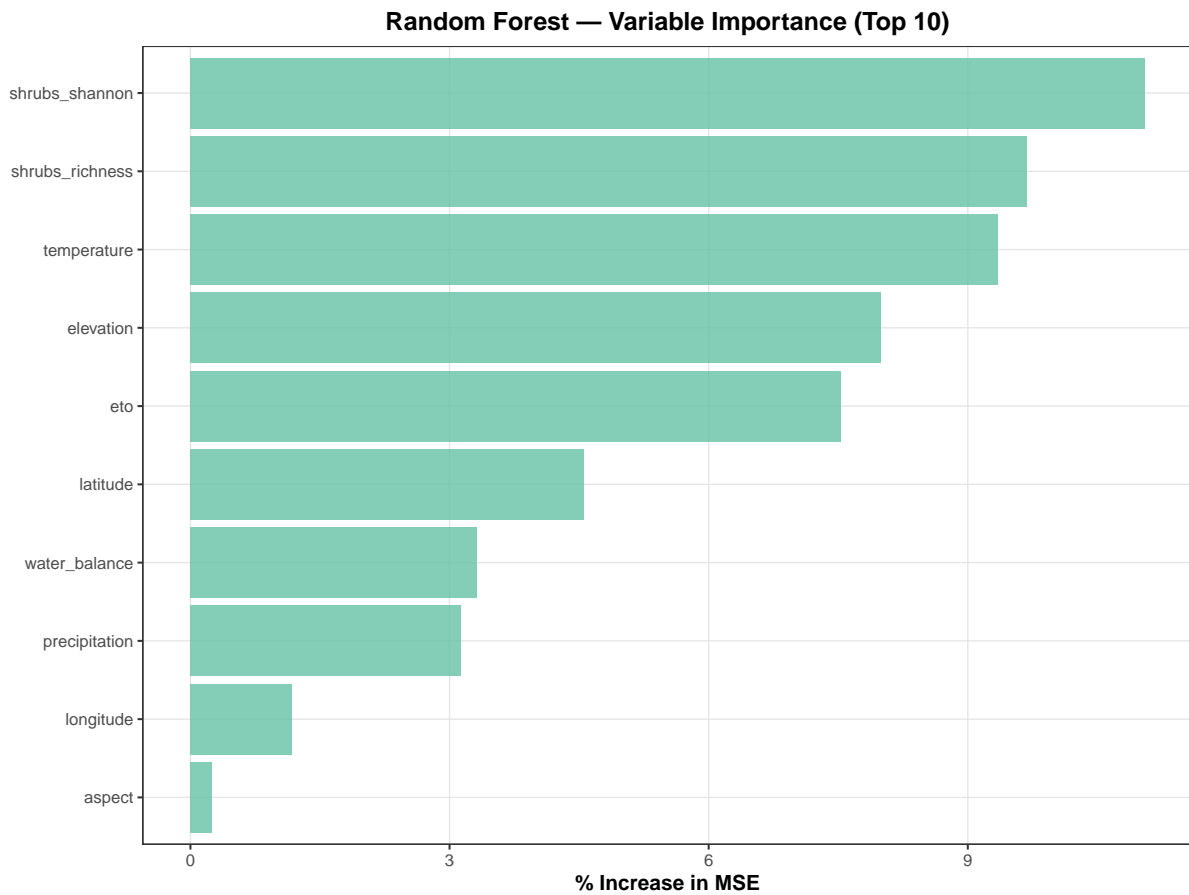


Figure 6: Random-forest variable-importance ranking for predictors of regeneration richness. Bars show percentage increase in mean squared error (%IncMSE) following permutation of each variable during five-fold cross-validation. Higher values indicate stronger influence on predictive accuracy.

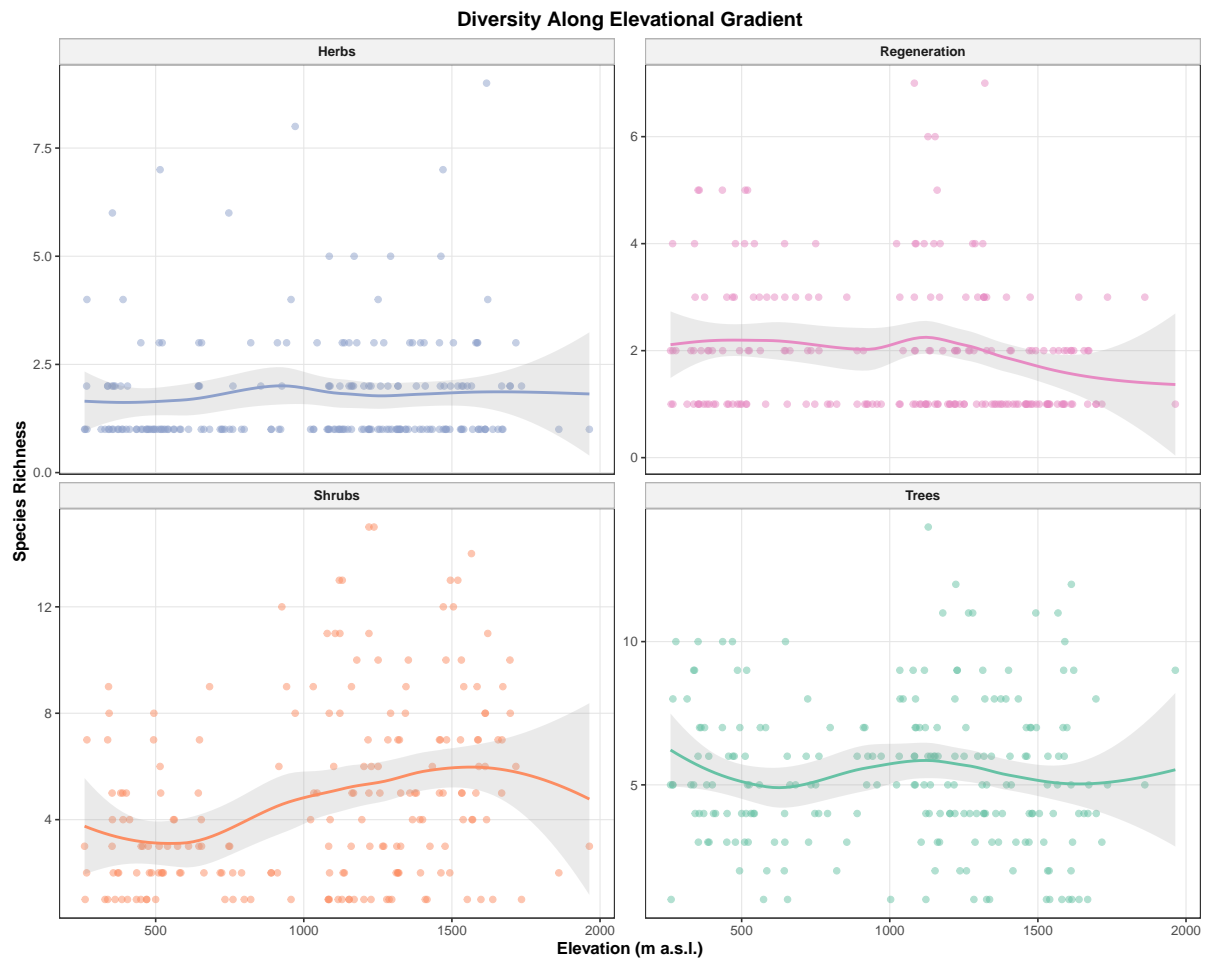


Figure 7: Variation in plot-level species richness along the elevational gradient for herbs, regeneration, shrubs and trees. Curves represent locally weighted regression fits with 95% confidence bands.

474 **Supporting Information**

475 Additional supporting information may be found online in the Supporting Information section:

476 Appendix S1. Variance inflation factor screening by stratum.

477 Appendix S2. Full PERMANOVA and dispersion outputs.

478 Appendix S3. Envfit results for all strata.

479 Appendix S4. Indicator species list.

480 Appendix S5. Machine-learning model parameters.

481 Appendix S6. Variable importance outputs.

482 Appendix S7. Cross-validation fold results.

483 Appendix S8. Diversity correlation matrix.

484 Appendix S9. Beta diversity metrics.

485 Appendix S10. Community matrix diagnostics.